

CARDIAC FUNCTION

Cardiac myosin binding protein-C Ser³⁰² phosphorylation regulates cardiac β -adrenergic reserveRanganath Mamidi,^{1*} Kenneth S. Gresham,^{2*} Jiayang Li,¹ Julian E. Stelzer^{1†}

Phosphorylation of cardiac myosin binding protein-C (MyBP-C) modulates cardiac contractile function; however, the specific roles of individual serines (Ser) within the M-domain that are targets for β -adrenergic signaling are not known. Recently, we demonstrated that significant accelerations in in vivo pressure development following β -agonist infusion can occur in transgenic (TG) mouse hearts expressing phospho-ablated Ser²⁸² (that is, TG^{S282A}) but not in hearts expressing phospho-ablation of all three serines [that is, Ser²⁷³, Ser²⁸², and Ser³⁰² (TG^{S302A})], suggesting an important modulatory role for other Ser residues. In this regard, there is evidence that Ser³⁰² phosphorylation may be a key contributor to the β -agonist-induced positive inotropic responses in the myocardium, but its precise functional role has not been established. Thus, to determine the in vivo and in vitro functional roles of Ser³⁰² phosphorylation, we generated TG mice expressing nonphosphorylatable Ser³⁰² (that is, TG^{S302A}). Left ventricular pressure-volume measurements revealed that TG^{S302A} mice displayed no accelerations in the rate of systolic pressure rise and an inability to maintain systolic pressure following dobutamine infusion similar to TG^{S302A} mice, implicating Ser³⁰² phosphorylation as a critical regulator of enhanced systolic performance during β -adrenergic stress. Dynamic strain-induced cross-bridge (XB) measurements in skinned myocardium isolated from TG^{S302A} hearts showed that the molecular basis for impaired β -adrenergic-mediated enhancements in systolic function is due to the absence of protein kinase A-mediated accelerations in the rate of cooperative XB recruitment. These results demonstrate that Ser³⁰² phosphorylation regulates cardiac contractile reserve by enhancing contractile responses during β -adrenergic stress.

INTRODUCTION

Activation of the β -adrenergic signaling pathway rapidly enhances ventricular contraction to increase cardiac output in response to enhanced systemic demand, via protein kinase A (PKA) activation, which phosphorylates key myofilament proteins involved in the regulation of myocardial force generation (1, 2). Previous studies have demonstrated that cardiac myosin binding protein-C (MyBP-C) phosphorylation regulates myofilament function by accelerating the rates of cross-bridge (XB) cycling and force generation in response to PKA treatment (3, 4). Animal models expressing phospho-ablated MyBP-C display an abolished PKA-mediated enhancement of the magnitude and rate of cooperative XB recruitment and force generation in skinned myocardium (5, 6), which limits the magnitude and the acceleration of left ventricular pressure generation in response to an acute β -agonist infusion (6–8). Thus, increased MyBP-C phosphorylation appears to be a primary mechanism by which the heart activates its contractile reserve under conditions of increased cardiac stress (7).

Despite growing evidence demonstrating the importance of MyBP-C phosphorylation in regulating in vivo cardiac contractile function, the respective roles of individual MyBP-C phosphorylation residues are not yet clear. In addition to PKA, which targets four M-domain MyBP-C residues (Ser²⁷³, Ser²⁸², Ser³⁰², and Ser³⁰⁷ mouse MyBP-C numbering) (9–13), individual MyBP-C residues are also selectively targeted by non-PKA kinases (9, 14). Previous studies have demonstrated a role for Ser²⁸² phosphorylation in accelerating XB recruitment and force generation (15, 16), which contributes to the in vivo acceleration of systolic pressure development following β -adrenergic stimulation

(16, 17). However, significant acceleration of in vivo pressure development was observed in Ser²⁸² phospho-ablated mice following infusion of the β -agonist dobutamine, whereas a complete MyBP-C phospho-ablation (that is, Ser²⁷³, Ser²⁸², and Ser³⁰²) abolished the acceleration in the rate of pressure development (6, 7, 16), demonstrating that phosphorylation of other PKA-targeted MyBP-C residues (Ser²⁷³ or Ser³⁰²) must be critical for modulation of the contractile response to increased β -adrenergic stimulation.

In addition to PKA, previous studies have shown that Ser³⁰² can be phosphorylated in vitro by several kinases, which are known to modulate cardiac function, such as PKC- ϵ (18), PKD (19), and glycogen synthase kinase-3 β (20). Furthermore, previous studies have suggested that increased Ca²⁺-dependent protein kinase II (CaMKII) activity due to increased cardiac pacing frequency enhances cardiac contractility, in part, due to increased Ser³⁰² phosphorylation (21). We have previously demonstrated that Ser³⁰² phosphorylation was lower than Ser²⁷³ or Ser²⁸² phosphorylation at baseline and was increased by PKA treatment to a greater extent than Ser²⁷³ and Ser²⁸² phosphorylation (7, 16). Thus, our hypothesis is that among MyBP-C phosphorylation residues, Ser³⁰² phosphorylation may be the principal MyBP-C residue, which modulates the inotropic contractile response to enhanced β -adrenergic activation, and that preventing Ser³⁰² phosphorylation impairs β -agonist-mediated enhancements in contractile response and reduces cardiac contractile reserve. However, to date, no study has examined the specific contribution of Ser³⁰² phosphorylation to in vivo contractile function. Therefore, to elucidate the precise roles of Ser³⁰² phosphorylation in modulating myofilament and in vivo contractile function, we generated a novel transgenic (TG) mouse model expressing MyBP-C with a nonphosphorylatable Ser³⁰² (that is, Ser³⁰² to Ala³⁰²; TG^{S302A}) and quantified the in vitro contractile response of skinned myocardium isolated from TG^{S302A} hearts to PKA treatment and in vivo contractile function of TG^{S302A} mice in response to β -agonist infusion.

¹Department of Physiology and Biophysics, School of Medicine, Case Western Reserve University, Cleveland, OH 44106, USA. ²Center for Translational Medicine, Temple University, Philadelphia, PA 19140, USA.

*These authors contributed equally to this work.

†Corresponding author. Email: julian.stelzer@case.edu

RESULTS

Sarcomeric protein expression and phosphorylation

To examine the role of MyBP-C Ser³⁰² phosphorylation in regulating β -adrenergic enhancement of ventricular contraction and relaxation, we generated a novel TG mouse line in which Ser³⁰² was mutated to an Ala residue to abolish phosphorylation (Fig. 1A). Expression of TG MyBP-C in TG^{S302A} myocardial samples was confirmed by Western blot analysis (Fig. 1B) and was detected as a full-length MyBP-C protein band at a molecular mass of ~150 kDa. Ser²⁷³ and Ser²⁸² phosphorylation was detected in TG^{S302A} samples and was similar to non-TG (NTG) phosphorylation (TG^{S302A} Ser²⁷³ phosphorylation was 106 \pm 6% and Ser²⁸² phosphorylation was 104 \pm 14% of NTG phosphorylation; $n = 5$), but Ser³⁰² phosphorylation was absent, confirming Ser³⁰² phospho-ablation in TG^{S302A} mice (Fig. 1B). TG MyBP-C expression in TG^{S302A} mice was determined to be 79 \pm 15% of NTG MyBP-C expression levels, similar to expression levels of MyBP-C TG mice in previous studies (6, 16). MyBP-C phosphorylation at Ser²⁷³, Ser²⁸², and Ser³⁰² was not detected in TG^{S3A} mice, as previously reported (Fig. 1B) (6, 7). The percentage of β -myosin heavy chain (MHC) expression in myocardium isolated from TG^{S302A} (3.6 \pm 1.5%) was found to be similar to NTG myocardium (2.2 \pm 1.2%), whereas β -MHC levels were slightly elevated in TG^{S3A} myocardium compared with NTG and TG^{S302A} myocardium (8.3 \pm 1.7%; $P < 0.05$) (Fig. 1C). The expression

and phosphorylation of other sarcomeric proteins, including troponin I (TnI), TnT, and regulatory light chain (RLC), were similar among all three groups (Fig. 1, D and E).

Following PKA treatment, Ser²⁷³ and Ser²⁸² phosphorylation levels were similar between TG^{S302A} and NTG samples (TG^{S302A} Ser²⁷³ phosphorylation was 97 \pm 10% and Ser²⁸² phosphorylation was 95 \pm 15% of PKA-treated NTG phosphorylation; $n = 3$ to 5), demonstrating normal PKA-mediated phosphorylation of these sites in the absence of Ser³⁰² phosphorylation (Fig. 1B). Ser³⁰² phosphorylation was not detected in TG^{S302A} samples following PKA treatment, confirming Ser³⁰² phospho-ablation. TnI and TnT phosphorylation levels were similar between TG^{S302A} and NTG samples following PKA treatment. Phosphorylation of RLC was unaffected by PKA treatment and was similar between TG^{S302A} and NTG samples under all conditions. Ser²⁷³, Ser²⁸², and Ser³⁰² phosphorylation was not detected in TG^{S3A} samples following PKA treatment. These results demonstrate that TG expression of S302A MyBP-C does not disrupt phosphorylation of other MyBP-C Ser residues or phosphorylation of other sarcomeric proteins.

Assessment of cardiac morphology

Representative formalin-fixed hearts and cross sections for NTG, TG^{S3A}, and TG^{S302A} hearts are presented in Fig. 2A. TG^{S302A} hearts exhibited similar overall size and morphology with no noticeable

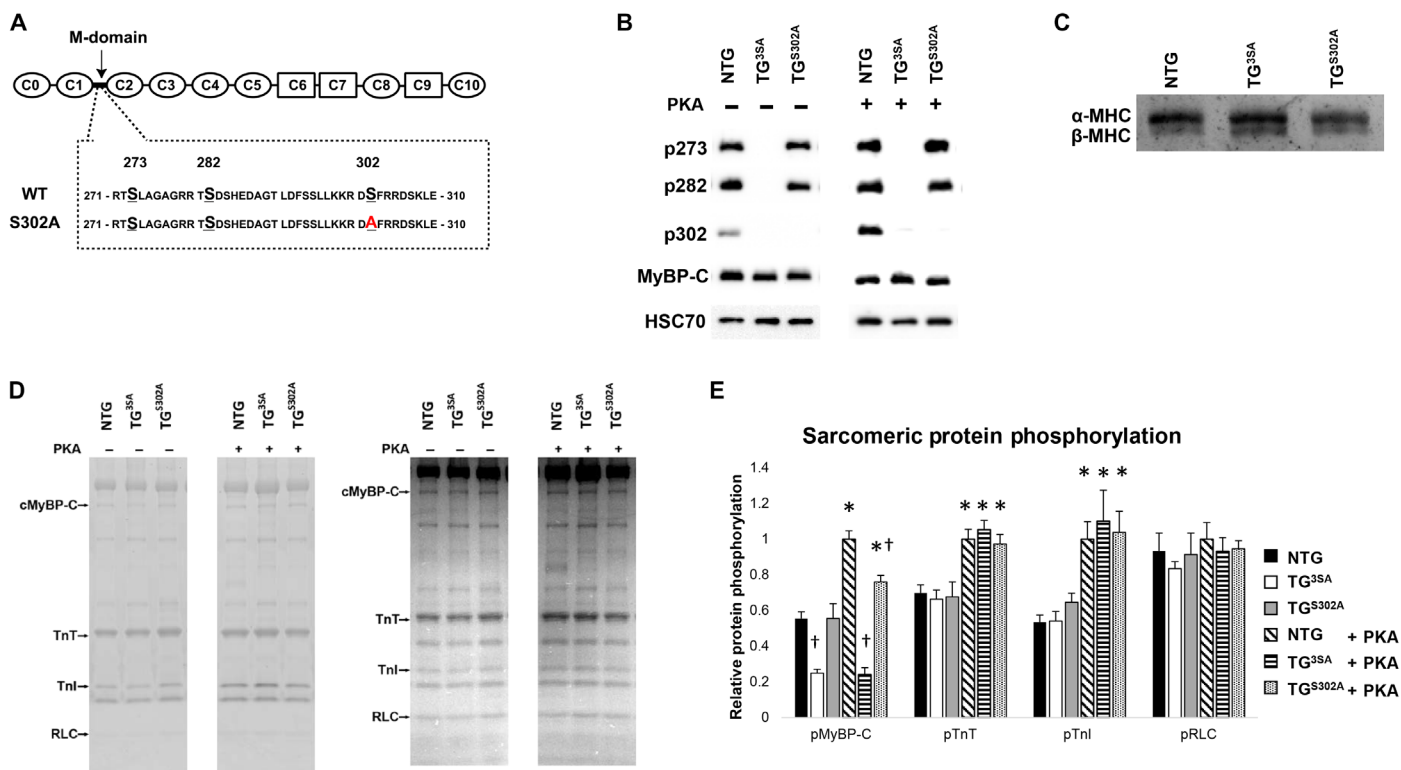


Fig. 1. Determination of expression, PKA-mediated phosphorylation of MyBP-C, and other sarcomeric proteins. (A) MyBP-C is composed of eight immunoglobulin (ovals) and three fibronectin III (rectangles) domains labeled C0 to C10 (N to C terminus). The conserved M-domain in the linker between domains C1 and C2 contains three serines (S273, S282, S302; mouse numbering) in the NTG sequence that are targets for PKA phosphorylation. The substitution used to prevent S302 phosphorylation in TG^{S302A} is shown in red. (B) Representative Western blot showing S273, S282, and S302 phosphorylation, before and after PKA incubation. No Ser³⁰² expression was detected in TG^{S302A} samples, whereas fully phosphorylatable Ser²⁷³ and Ser²⁸² were observed. (C) Representative 5% tris-HCl gel, stained with silver stain, showing MHC isoform expression in the myocardial samples. (D) Representative gels shown are stained by Pro-Q (left) for protein phosphorylation, and the same gel is shown for total protein (right) stained with Coomassie Blue. cMyBP-C, cardiac myosin binding protein-C; pMyBP-C, phosphorylated cardiac myosin binding protein-C. (E) Relative protein phosphorylation (phosphorylated signal/total protein signal) was calculated for each protein and is expressed as % of PKA-treated NTG values for that protein. Values are expressed as means \pm SEM, from three to six hearts in each group. * $P < 0.05$, different from non-PKA-treated samples from the same line; † $P < 0.05$, different from the corresponding NTG group.

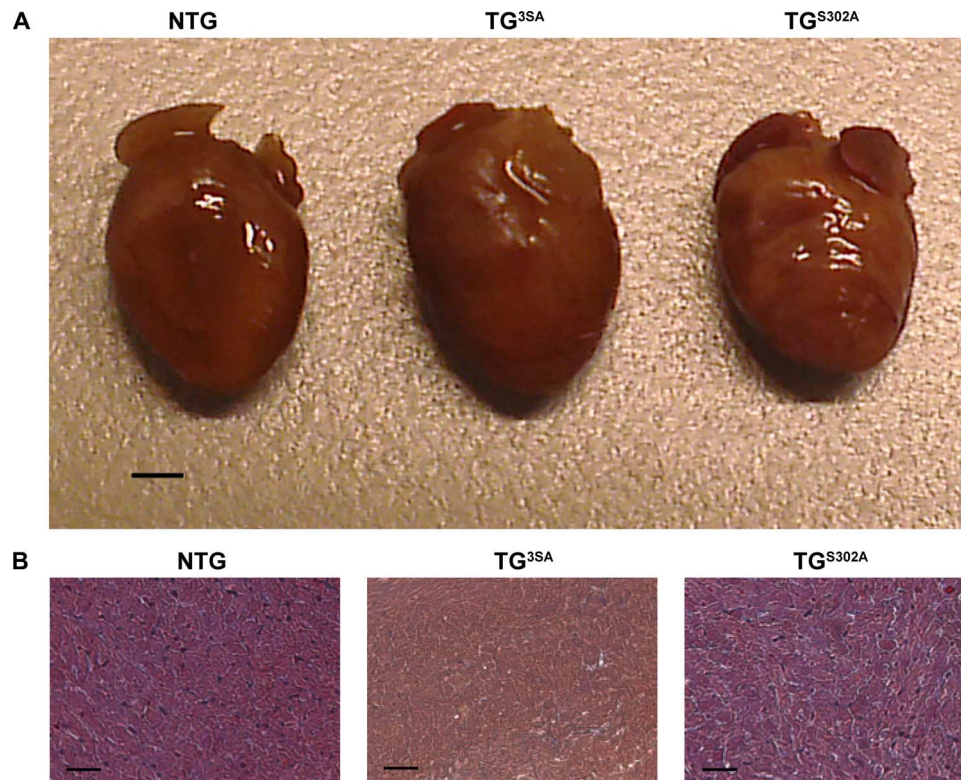


Fig. 2. Analysis of cardiac morphology. (A) Representative NTG, TG^{35A}, and TG^{S302A} formalin-fixed hearts. TG^{S302A} hearts showed a similar overall morphology compared to NTG hearts, in contrast to the enlarged heart size observed in TG^{35A} hearts. Scale bar, 1 mm. (B) Representative cross sections of NTG, TG^{35A}, and TG^{S302A} hearts from the mid-LV were stained with Masson's trichrome and imaged at $\times 100$ magnification, demonstrating no observable increase in fibrosis in TG^{S302A} hearts. Scale bars, 25 μ m.

alterations in chamber geometry or increased cardiac fibrosis (Fig. 2B) when compared to control NTG hearts. In contrast to the cardiac hypertrophy produced by complete MyBP-C phospho-ablation (Fig. 2 and Table 1), left ventricle (LV) mass and wall thickness were similar between TG^{S302A} and NTG mice as measured by echocardiography. These results demonstrate that Ser³⁰² phospho-ablation does not result in pathological cardiac hypertrophy.

Basal cardiac function

Cardiac contractile and hemodynamic function was assessed by echocardiography and pressure-volume (P-V) loop analysis to determine the functional effects of Ser³⁰² phospho-ablation. No changes in systolic function or diastolic function as evidenced by measurements of ejection fraction (EF) or isovolumic relaxation time (IVRT) were detected in TG^{S302A} mice compared to NTG controls (Table 1). Similarly, no differences were detected in the rate of pressure development (dp/dt_{max}) or relaxation (τ) at baseline between TG^{S302A} mice and NTG controls (Table 2). In contrast, complete MyBP-C phospho-ablation in TG^{35A} hearts resulted in slowed IVRT and reduced EF at baseline (Table 1), consistent with previous studies (6, 7, 22).

β -Adrenergic reserve

The contribution of Ser³⁰² phosphorylation to the contractile response to β -adrenergic stimulation was assessed in TG^{S302A} mice following dobutamine infusion. The postdobutamine dp/dt_{max} in TG^{S302A} mice was slower than in dobutamine-treated NTG mice ($P < 0.005$; Table 2 and Fig. 3A), and the rate of pressure development throughout early systole in dobutamine-treated TG^{S302A} mice was lower when compared to the

Table 1. LV morphology and in vivo cardiac performance measured by echocardiography. BW, body weight; LV mass/BW, ratio of LV and body weight; HR, heart rate; PWd, posterior wall thickness in diastole; PWs, posterior wall thickness in systole; IVRT, isovolumic relaxation time; EF, ejection fraction. Values are expressed as means \pm SEM from 10 mice per group.

	NTG	TG ^{35A}	TG ^{S302A}
BW (g)	27.5 \pm 0.5	26.2 \pm 1.3	26.9 \pm 0.6
LV mass/BW	3.8 \pm 0.2	5.8 \pm 0.4*	4.0 \pm 0.2
HR (beats/min)	418 \pm 8	431 \pm 13	425 \pm 10
PWd (mm)	0.88 \pm 0.01	1.13 \pm 0.03*	0.91 \pm 0.02
PWs (mm)	1.18 \pm 0.03	1.39 \pm 0.1*	1.23 \pm 0.02
IVRT (ms)	18.1 \pm 1.5	28.5 \pm 2.1*	19.4 \pm 1.4
EF (%)	75.1 \pm 2.6	62.0 \pm 2.2*	73.1 \pm 2.2

* $P < 0.05$, different compared to NTG.

rate of pressure development observed in dobutamine-treated NTG mice (Fig. 3B), demonstrating that Ser³⁰² phosphorylation is required to accelerate pressure development following β -adrenergic stimulation. The acceleration in pressure development in NTG mice following dobutamine increased early systolic developed pressure levels compared to baseline (Fig. 3), but the impaired acceleration in pressure development

Table 2. Left ventricular hemodynamic function measured by P-V loop analysis. HR, heart rate; P_{max} , maximal systolic pressure; EDP, end diastolic pressure; dP/dt_{max} , maximum rate of pressure development; τ , time constant of pressure relaxation; DOB, dobutamine. Values are expressed as means \pm SEM. $n = 9$ for NTG, 8 for TG^{35A} , and 10 for TG^{S302A} .

Group	HR (beats/min)	P_{max} (mmHg)	EDP (mmHg)	dP/dt_{max} (mmHg/s)	τ (ms)
- DOB					
NTG	456 \pm 11	95.3 \pm 3.7	6.1 \pm 0.9	7,487 \pm 512	8.1 \pm 0.3
TG^{35A}	451 \pm 11	87.7 \pm 3.1	6.2 \pm 1.1	7,216 \pm 290	9.2 \pm 0.6
TG^{S302A}	470 \pm 5	92.9 \pm 3.4	6.4 \pm 0.6	6,690 \pm 401	8.5 \pm 0.3
+ DOB					
NTG	537 \pm 7*	96.9 \pm 3.4	4.8 \pm 0.6*	13,962 \pm 919*	6.7 \pm 0.4*
TG^{35A}	531 \pm 9*	85.0 \pm 2.6†	4.4 \pm 0.4	8,141 \pm 652†	8.8 \pm 0.6†
TG^{S302A}	553 \pm 6*	87.0 \pm 1.9†	3.7 \pm 0.2*	8,725 \pm 337††	6.9 \pm 0.5*

* $P < 0.05$, different versus the corresponding baseline group (without dobutamine). † $P < 0.05$, different versus the corresponding NTG group.

in TG^{S302A} mice prevented an increase in developed pressure, resulting in developed pressure levels that were similar to NTG mice before dobutamine treatment (Fig. 3). Additionally, maximal systolic pressure was lower in TG^{S302A} mice following dobutamine treatment compared to NTG controls ($P < 0.005$; Table 2). The impaired acceleration in pressure development and decreased maximal systolic pressure observed in TG^{S302A} mice were also observed in TG^{35A} mice, consistent with our previous study (7). There were no differences in the rate or magnitude of pressure development following dobutamine treatment between TG^{35A} and TG^{S302A} mice (Table 2), suggesting that phosphorylation of Ser²⁷³ and Ser²⁸² cannot compensate for the loss of Ser³⁰² phosphorylation following β -adrenergic stimulation. Similar to previous reports of individual MyBP-C Ser residue phospho-ablation (16), Ser³⁰² phospho-ablation did not disrupt normal acceleration of diastolic pressure relaxation because dobutamine accelerated relaxation to a similar extent in TG^{S302A} and NTG mice (Table 2), in contrast to TG^{35A} mice, which displayed slowed relaxation following dobutamine treatment.

Basal myofilament contractile function

The effects of Ser³⁰² phospho-ablation on myofilament contractile properties were assessed in skinned myocardium isolated from TG^{S302A} hearts (Fig. 4, A to D). Stretch activation experiments were performed to measure dynamic strain-induced XB behavior. Figure 4 illustrates a

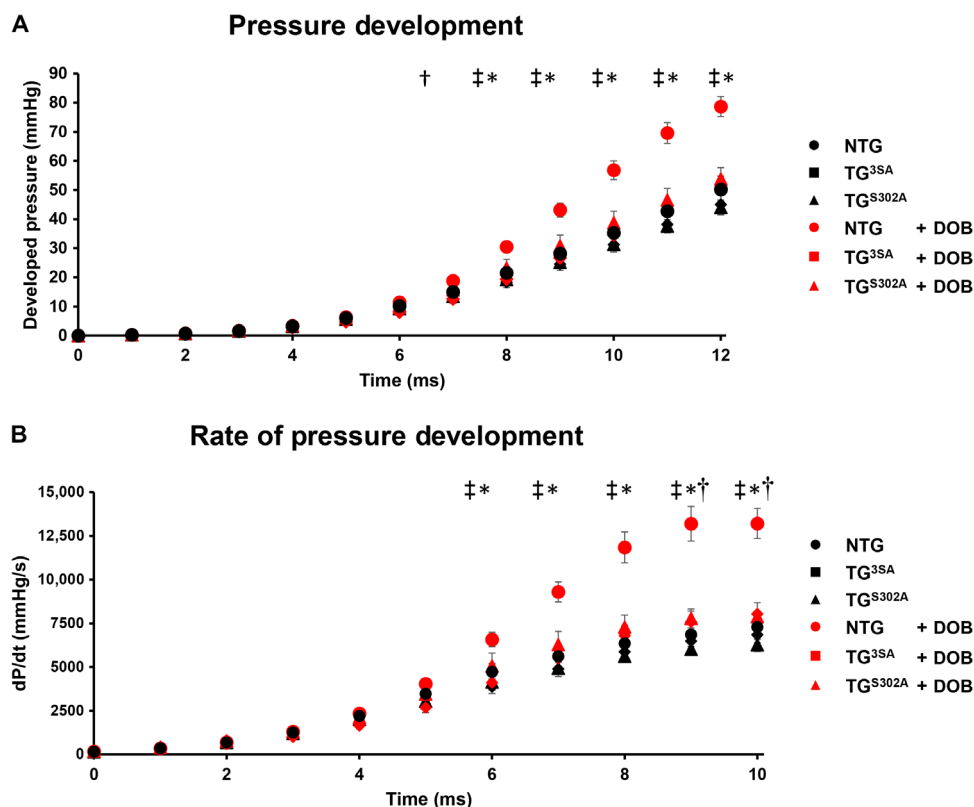


Fig. 3. Analysis of the β -adrenergic acceleration in pressure development. (A) Developed pressure, where end diastolic pressure was subtracted from instantaneous ventricular pressure, was plotted during early systolic contraction, to yield developed pressure. Dobutamine (DOB) increased the developed pressure in NTG mice starting at 8 ms after the start of contraction compared to baseline ($P = 0.015$) but did not increase developed pressure in TG^{35A} or TG^{S302A} mice. Following dobutamine treatment, developed pressure in TG^{S302A} mice was not higher than that in NTG mice before dobutamine treatment at any point examined (that is, NTG at baseline). (B) The rate of pressure development (dP/dt) was measured during early systole. Dobutamine accelerated dP/dt starting at 6 ms after the start of contraction in NTG ($P < 0.005$). In TG^{S302A} mice, the acceleration in dP/dt was blunted compared to that in NTG mice and was only faster than baseline after 9 ms ($P < 0.05$). dP/dt in TG^{S302A} mice was not faster after dobutamine than NTG dP/dt before dobutamine treatment (that is, NTG at baseline) at any time point examined. * $P < 0.05$, NTG + dobutamine versus NTG without dobutamine treatment; † $P < 0.05$, TG^{S302A} + dobutamine versus TG^{S302A} without dobutamine treatment; ‡ $P < 0.05$, NTG + dobutamine versus TG^{S302A} + dobutamine.

typical stretch activation response in skinned myocardium isolated from NTG, TG^{3SA}, and TG^{S302A} hearts and highlights the parameters assessed in the resultant force transients following the imposed stretch. Under basal conditions, the rate of delayed force development following the imposed stretch (that is, k_{df}) and the magnitude of XB recruitment (that is, P_{df}) were not different between the NTG and TG^{S302A} groups, whereas TG^{3SA} myocardium displayed diminished P_{df} (Table 3). However, the rate of force decay (k_{rel}) in TG^{S302A} myocardium was slower than that in NTG myocardium ($P = 0.01$) and was not different from TG^{3SA} skinned myocardium (Table 3). Additionally, P2 values in TG^{S302A} skinned myocardium were higher than those in NTG myocardium ($P = 0.03$) and were similar to TG^{3SA} values, indicating that the magnitude of strain-induced XB detachment was lower in the TG^{S302A} and TG^{3SA} groups. No differences in Ca²⁺-activated maximal force (F_{max}), Ca²⁺-independent force (F_{min}), Ca²⁺ sensitivity of force development (pCa₅₀), or cooperativity of force development (n_H) were observed between the NTG, TG^{3SA}, and TG^{S302A} groups (Table 4), indicating that differences in dynamic XB behavior were not due to changes in Ca²⁺-mediated thin filament activation.

Myofilament contractile function following PKA treatment

Following PKA treatment, both TG^{S302A} and TG^{3SA} skinned myocardium displayed slower rates of stretch-induced delayed force develop-

ment (k_{df}) compared to NTG myocardium (Table 3 and Fig. 4D). PKA treatment accelerated k_{df} by $\sim 65 \pm 17\%$ ($P < 0.005$) in NTG myocardium but had no effect on k_{df} in TG^{S302A} or TG^{3SA} myocardium, demonstrating that Ser³⁰² phospho-ablation impairs PKA-mediated accelerations in the rate of XB recruitment to the same extent as complete MyBP-C phospho-ablation. Following PKA incubation, P3 was increased by $\sim 43 \pm 9\%$ ($P < 0.005$) and $\sim 25 \pm 6\%$ ($P = 0.005$) in the NTG and TG^{S302A} groups but not in the TG^{3SA} group (Fig. 5A). TG^{S302A} skinned myocardium also displayed an impaired magnitude of XB recruitment (P_{df}) following PKA treatment compared to NTG myocardium (Table 3). Whereas P_{df} was increased by PKA incubation by $\sim 84 \pm 14\%$ ($P < 0.005$), $\sim 61 \pm 12\%$ ($P < 0.005$), and $\sim 61 \pm 9\%$ ($P < 0.005$) in the NTG, TG^{3SA}, and TG^{S302A} groups (Fig. 5B), respectively (Table 3), P_{df} was higher in the NTG group compared to the TG^{S302A} group ($P < 0.005$), demonstrating that Ser³⁰² phospho-ablation blunts the PKA-mediated enhancement in the overall magnitude of XB recruitment.

In addition to enhancing the rate of delayed force development, PKA treatment also accelerated the rate and magnitude of force decay following stretch. In NTG myocardium, PKA treatment accelerated the rate of force decay ($\sim 80 \pm 13\%$ increase in k_{rel} ; $P < 0.005$) and produced a greater magnitude of force decay (that is, more negative P2 values). However, the PKA-mediated acceleration in force decay was

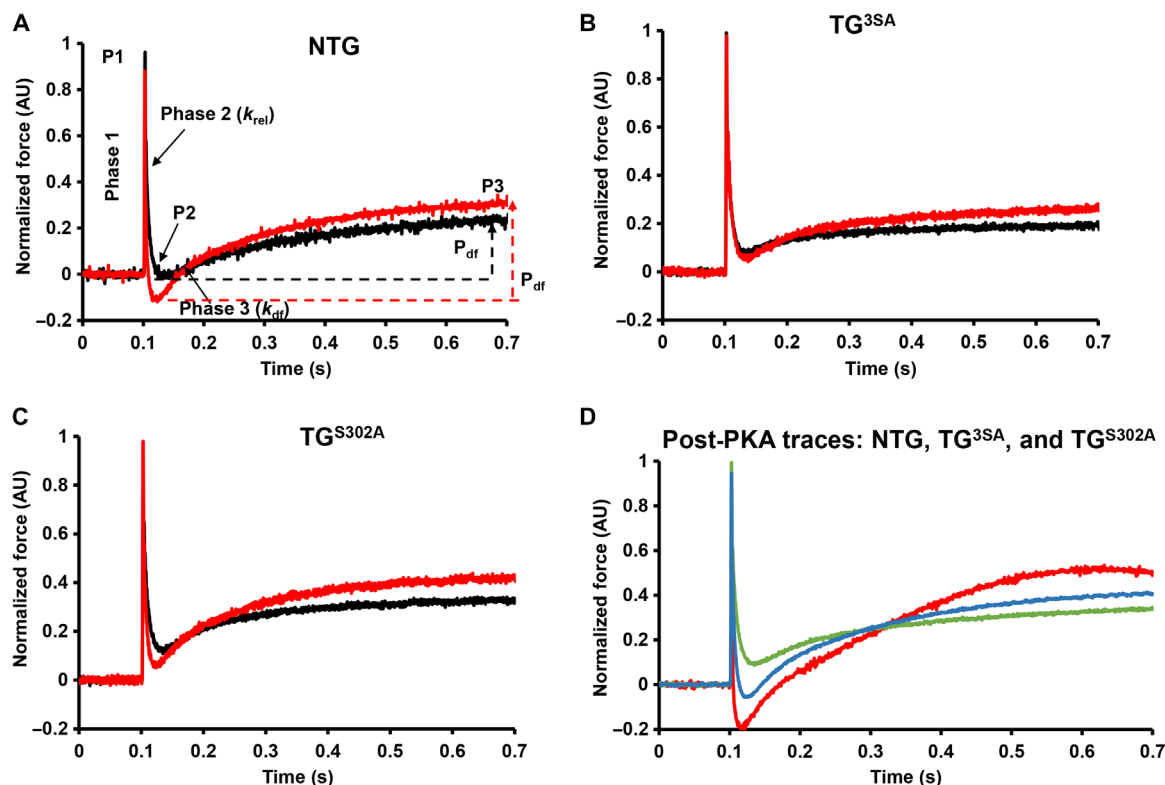


Fig. 4. Effect of PKA treatment on the stretch activation responses in NTG, TG^{3SA}, and TG^{S302A} skinned myocardium. Representative force responses elicited by a sudden 2% stretch in muscle length (ML) in isometrically contracting (A) NTG, (B) TG^{3SA}, and (C) TG^{S302A} myocardial preparations before (black) and following (red) PKA incubation. (D) Representative stretch activation traces following PKA treatment for NTG (red), TG^{3SA} (green), and TG^{S302A} (blue) myocardial preparations. Following PKA treatment, NTG preparations exhibited faster XB contractile behavior, whereas TG^{3SA} exhibited slower XB contractile behavior and TG^{S302A} exhibited intermediate XB contractile behavior. In (A), highlighted are the important phases of the force transients and the various stretch activation parameters that are derived from the elicited force response (see Materials and Methods for explanation of each phase and parameters). PKA incubation accelerated both k_{rel} ($P < 0.005$) and k_{df} ($P < 0.005$) in NTG skinned myocardium. However, in the TG^{S302A} skinned myocardium, the PKA-mediated acceleration in k_{rel} is less pronounced ($P = 0.02$) than that in the NTG coupled with no PKA-mediated accelerations in k_{rel} and k_{df} in TG^{3SA} skinned myocardium. AU, arbitrary units.

Table 3. Dynamic stretch-activation parameters measured in NTG, TG^{35A}, and TG^{S302A} skinned myocardium. Twelve preparations isolated from four hearts were used for all the groups. P1, XB stiffness; P2, magnitude of XB detachment; P3, the new steady-state force attained in response to the imposed stretch in ML; P_{df} , magnitude of XB recruitment; P_0 , prestretch isometric force; k_{rel} , rate of XB detachment; k_{df} , rate of XB recruitment. Values are expressed as means \pm SEM.

Group	P1 (P1/ P_0)	P2 (P2/ P_0)	P3 (P3/ P_0)	P_{df}	k_{rel} (s ⁻¹)	k_{df} (s ⁻¹)
- PKA						
NTG	0.558 \pm 0.013	-0.026 \pm 0.010	0.189 \pm 0.012	0.215 \pm 0.021	497.33 \pm 40.51	5.24 \pm 0.51
TG ^{35A}	0.564 \pm 0.031	0.053 \pm 0.015*	0.175 \pm 0.012	0.123 \pm 0.016*	314.38 \pm 25.85*	5.31 \pm 0.34
TG ^{S302A}	0.537 \pm 0.018	0.016 \pm 0.014*	0.183 \pm 0.013	0.167 \pm 0.020	355.36 \pm 34.10*	6.15 \pm 0.51
+ PKA						
NTG	0.466 \pm 0.011†	-0.106 \pm 0.011†	0.265 \pm 0.017†	0.371 \pm 0.023†	874.41 \pm 77.10†	7.85 \pm 0.44†
TG ^{35A}	0.513 \pm 0.026	0.013 \pm 0.013*	0.203 \pm 0.016*	0.190 \pm 0.023*†	346.91 \pm 37.46*	4.85 \pm 0.35*
TG ^{S302A}	0.521 \pm 0.017	-0.024 \pm 0.019*†	0.227 \pm 0.016†	0.251 \pm 0.019*†‡	509.89 \pm 52.27*†‡	6.20 \pm 0.50*‡

*Different versus the corresponding NTG group. †Different versus the corresponding (-PKA) group, $P < 0.05$. ‡Different versus the corresponding TG^{35A} group.

blunted in TG^{S302A} myocardium ($\sim 45 \pm 8\%$ increase in k_{rel} ; $P < 0.005$) and resulted in k_{rel} values similar to pre-PKA k_{rel} values in NTG skinned myocardium (Table 3), suggesting that Ser³⁰² phosphorylation is required for complete acceleration of the rate of XB detachment following PKA treatment. PKA incubation also decreased P2 values in the TG^{S302A} group but to a lesser extent than in the NTG group (Table 3). PKA treatment did not accelerate k_{rel} (Fig. 5C) or decrease P2 amplitude in TG^{35A} myocardium when compared to the NTG group, as previously reported (5).

PKA treatment similarly decreased the pCa_{50} in all the groups, and no differences were observed in F_{max} , F_{min} , and n_H between groups before or following PKA treatment (Table 4). Therefore, our data indicate that Ser³⁰² phospho-ablation does not affect the Ca²⁺-sensitivity of force generation and that the impaired acceleration in force decay and delayed force development in TG^{S302A} skinned myocardium are due to a diminished PKA-mediated enhancement of XB kinetics in the absence of Ser³⁰² phosphorylation.

DISCUSSION

Although augmented ventricular function during β -adrenergic stimulation requires MyBP-C phosphorylation, it is unclear how Ser³⁰² phos-

phorylation contributes to enhanced myofilament and whole-heart contractile function. Therefore, to define the effects of Ser³⁰² phosphorylation on in vitro and in vivo contractile function, we generated novel TG mice expressing nonphosphorylatable MyBP-C Ser³⁰² (that is, TG^{S302A}). Our findings show that Ser³⁰² phospho-ablation did not disrupt PKA-mediated phosphorylation of neighboring MyBP-C Ser residues (that is, 273 and 282) or other sarcomeric proteins and did not induce significant maladaptive cardiac remodeling or altered basal ventricular function. However, Ser³⁰² phospho-ablation largely prevented β -adrenergic enhancement of the rate of systolic pressure development and decreased maximal systolic pressure following β -adrenergic stimulation, demonstrating that Ser³⁰² phosphorylation is the predominant MyBP-C residue responsible for regulation of cardiac systolic β -adrenergic reserve. Measurements of dynamic XB behavior revealed that loss of β -adrenergic reserve at the whole-heart level was mirrored by the loss of PKA-mediated accelerations in cooperative XB recruitment into the force-generating states at the myofilament level. Collectively, our data show that MyBP-C Ser³⁰² phosphorylation is required to enhance force and pressure generation during enhanced β -adrenergic signaling and uniquely equips the heart with a functional reserve to meet higher circulatory demands during β -adrenergic stimulation.

Table 4. Steady-state contractile parameters measured in NTG, TG^{35A}, and TG^{S302A} skinned myocardium. F_{min} , Ca^{2+} -independent force measured at pCa 9.0; F_{max} , Ca^{2+} -activated maximal force measured at pCa 4.5; n_{H} , Hill coefficient of the force-pCa relationship; pCa₅₀, pCa required for the generation of half-maximal force. Values are expressed as means \pm SEM.

Group	F_{min} (mN/mm ²)	F_{max} (mN/mm ²)	n_{H}	pCa ₅₀
– PKA				
NTG	1.21 \pm 0.13	17.21 \pm 2.05	2.50 \pm 0.15	5.86 \pm 0.02
TG ^{35A}	1.48 \pm 0.18	20.44 \pm 2.47	2.66 \pm 0.27	5.88 \pm 0.01
TG ^{S302A}	1.18 \pm 0.20	17.46 \pm 2.48	2.37 \pm 0.15	5.89 \pm 0.01
+ PKA				
NTG	1.10 \pm 0.16	17.86 \pm 1.78	2.87 \pm 0.16	5.75 \pm 0.01*
TG ^{35A}	1.17 \pm 0.21	20.77 \pm 3.54	2.80 \pm 0.20	5.77 \pm 0.02†
TG ^{S302A}	1.07 \pm 0.23	16.25 \pm 2.39	2.42 \pm 0.17	5.78 \pm 0.02*

*Different versus the corresponding (– PKA) group; †12 preparations isolated from four hearts were used for all the groups.

Ser³⁰² phosphorylation is required for complete cooperative recruitment of XBs during submaximal Ca^{2+} activation

MyBP-C Ser³⁰² phosphorylation is relatively lower than Ser²⁷³ and Ser²⁸² under basal conditions but is highly phosphorylated following PKA incubation (16, 23); therefore, it is expected that MyBP-C Ser³⁰² phosphorylation substantially contributes to enhanced contractile performance following β -adrenergic stimulation. Our data show that TG^{S302A} skinned myocardium displayed a slowed rate and diminished magnitude of XB detachment (k_{rel} and P2), along with a reduced magnitude of cooperative XB recruitment (P_{df}) compared to NTG skinned myocardium, suggesting that ablation of even low levels of basal Ser³⁰² phosphorylation impairs dynamic XB behavior (Table 3). Following PKA incubation, functional differences between TG^{S302A} and NTG skinned myocardium were amplified. Although we observed PKA-induced accelerations in k_{rel} and enhancements in P2 (indicating increases in both the rate and magnitude of XB detachment in TG^{S302A} skinned myocardium), the effects were smaller than NTG skinned myocardium (Table 3 and Fig. 4). Notably, unlike NTG skinned myocardium, following PKA incubation, TG^{S302A} skinned myocardium did not display significant accelerations in k_{df} , an indicator of the rate of cooperative XB recruitment into the force-generating XB pool. This finding is in agreement with an earlier study, which showed that selective phosphorylation of Ser³⁰² by PKD accelerates the rate of tension redevelopment in wild-type mouse myocardium (19). Additionally, PKA-induced enhancement in P_{df} , which is an indicator of the magnitude of XB recruitment into the force-generating XB pool, was also blunted in TG^{S302A} skinned myocardium when compared to the NTG skinned myocardium, indicating that Ser³⁰² phosphorylation modulates the overall number of cooperatively recruited force-generating XBs during PKA-mediated myofilament activation. Previous studies using intact mouse papillary fibers showed that increased pacing frequency (an activator of CaMKII δ , which targets Ser³⁰² primarily and Ser²⁸² to a lesser degree) accelerates the rates of force development and relaxation in wild-type fibers but these responses are diminished in TG^{35A} fibers, indicating that phospho-ablation of

MyBP-C depresses CaMKII δ -mediated enhancements in contractile function (21). However, under normal physiological conditions, the immediate/short-term demand for increased cardiac inotropy is primarily met by PKA activation, which provides an acute boost in contractility due to phosphorylation of all three Ser residues, whereas the need for prolonged increases in cardiac contractile function [that is, prolonged increases in pacing frequency (21)] may be met by increased CaMKII activation, which phosphorylates only a subset of Ser residues (24). Thus, it is likely that PKA-mediated Ser³⁰² phosphorylation is the main contributor to β -adrenergic stimulation-mediated enhancements in cardiac contractility under normal physiological conditions.

The magnitude of cooperative XB recruitment and binding to the thin filaments is influenced both by Ca^{2+} binding to TnC and by XB binding to actin. Ca^{2+} binding to TnC rapidly turns on the thin filament regulatory units and opens up the myosin binding sites on actin by displacing the tropomyosin to facilitate XB binding, which allows for propagation of XB-mediated cooperative XB recruitment along neighboring thin filament regulatory units (25). Cooperative XB-mediated recruitment of additional XBs is further facilitated by PKA phosphorylation of MyBP-C (26), which accelerates XB transitions to force-bearing states and enhances the probability of actomyosin interactions by displacing and orienting the XBs away from the thick filament backbone toward the actin sites (27) and also by reducing XB on time, which allows for accelerated XB turnover and recruitment of additional XBs to vacated myosin binding sites on actin (26). The mechanism by which MyBP-C phosphorylation enhances cooperative XB recruitment may be due to enhanced thin filament activation upon binding of phosphorylated MyBP-C to actin, which induces displacement of tropomyosin to the open state (28), or due to reduced binding of MyBP-C to myosin S2, which facilitates XB binding to actin (29–32), or both. Thus, at submaximal Ca^{2+} activations, MyBP-C phosphorylation not only accelerates the rate of force development but also expands the spread of thin filament activation beyond regulatory units that have already been activated by Ca^{2+} , thereby shifting the net equilibrium of myosin XBs toward the force-bearing states and greatly enhancing myocardial force generation (26). In contrast, a reduction in MyBP-C Ser³⁰² phosphorylation would be expected to slow cooperative XB recruitment and turnover, thereby disrupting the equilibrium of XB transitions into the force-generating pool, which in turn limits systolic pressure generation during β -adrenergic stimulation. However, as the level of Ca^{2+} -activation increases, myofilament force generation becomes less reliant on cooperative XB recruitment because more thin filament regulatory units are directly activated by Ca^{2+} , and thus, the modulatory influence of MyBP-C phosphorylation on XB behavior diminishes (5, 12).

MyBP-C Ser³⁰² phosphorylation is required to enhance systolic pressure development

Although all three M-domain MyBP-C residues are targets of PKA phosphorylation, Ser³⁰² phosphorylation is observed at low levels in vivo and is lower than the other two PKA-targeted sites, Ser²⁷³ and Ser²⁸² (16, 23). Because the pool of MyBP-C that can be phosphorylated at Ser³⁰² following β -adrenergic stimulation (~95% of total MyBP-C) is larger than for Ser²⁷³ and Ser²⁸², loss of phosphorylation at Ser³⁰² would be expected to reduce the recruitable pool of force-generating XBs to a greater extent than loss of phosphorylation at the other PKA sites in response to β -adrenergic signaling. The rate of pressure development and maximal developed pressure were not different between TG^{35A} and TG^{S302A} mice following dobutamine treatment, suggesting

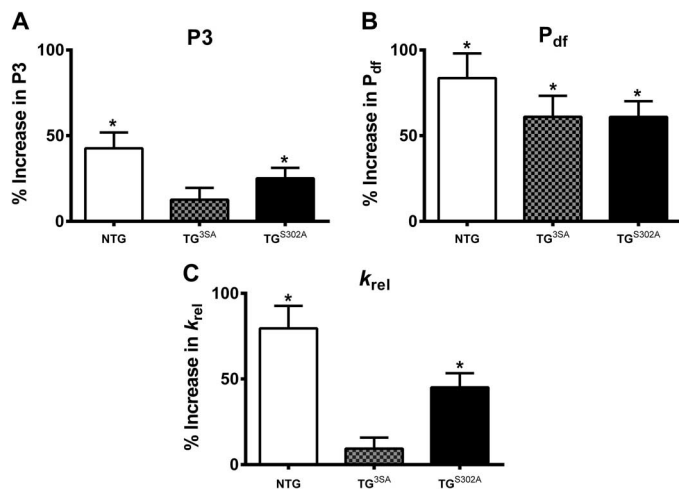


Fig. 5. Effect of PKA on stretch activation parameters. Measurements in the skinned ventricular preparations were first made under basal conditions (no PKA). Measurements were again made on the same preparations following PKA incubation. The net changes in stretch activation parameters after PKA incubation were calculated and are expressed as % increases from baseline for (A) the magnitude of new steady-state force attained in response to stretch in ML, P₃; (B) the magnitude of overall XB recruitment in response to stretch in ML, P_{drf} and (C) the rate of XB detachment, k_{rel} in the NTG, TG^{35A}, and TG^{302A} groups. PKA treatment enhanced the P_{drf} in all the groups, but the PKA-mediated enhancements in P_{drf} were lower in the TG^{35A} and TG^{302A} groups when compared to the NTG group, indicating that the magnitude of XB recruitment occurs to a lesser extent in the TG^{35A} and TG^{302A} groups. NTG preparations displayed accelerations in k_{rel} following PKA incubation; however, this acceleration in k_{rel} was less pronounced in the TG^{302A} group and is completely absent in the TG^{35A} group. Similar effects were observed for P₃. Values are expressed as means ± SEM. *P < 0.05; 12 preparations isolated from four hearts were used for all the groups.

that phosphorylation of Ser³⁰² was needed to recruit the reserve force-generating XBs to enhance pressure development above basal levels. Previous studies have suggested that in addition to the known PKA phosphorylation residues Ser²⁷³, Ser²⁸², and Ser³⁰², a fourth residue, Ser³⁰⁷, may also be a target of PKA phosphorylation (9–13). However, TG^{35A} hearts did not exhibit systolic enhancements following dobutamine treatment despite expressing a phosphorylatable Ser³⁰⁷ residue, suggesting that Ser³⁰⁷ is unlikely to be involved in modulating the molecular and in vivo behaviors that we measured in this study. Together, our data suggest that Ser³⁰² is the primary MyBP-C residue that modulates the positive inotropic response to enhanced β-adrenergic stimulation.

By preventing the recruitment of additional XBs following β-adrenergic stimulation, Ser³⁰² phospho-ablation slowed pressure development and reduced maximal systolic pressure development without disrupting basal systolic pressure development. Loss of phosphorylation at Ser³⁰² did not produce pathological cardiac hypertrophy or notable changes in basal unstressed ventricular function, perhaps because the primary role of Ser³⁰² phosphorylation is to promote greater XB recruitment at higher workloads when β-adrenergic signaling is enhanced. This is also consistent with the observation that myocardial force generation is unaltered at baseline but cannot be enhanced by PKA or CaMKII (which targets Ser³⁰²) in myocardium expressing nonphosphorylatable MyBP-C (21) because the reserve pool of recruitable XBs is reduced by Ser³⁰² phospho-ablation.

It was proposed that Ca²⁺ is released from ryanodine receptors near the Z line in myocytes and diffuses toward the center of the sarcomere (13): first, activating thin filament regulatory units in the region of the

sarcomere that does not contain MyBP-C and, subsequently, activating the thin filament in MyBP-C-containing regions. Increased Ca²⁺ release following β-adrenergic stimulation would be expected to increase XB recruitment, in part, by increasing thin filament activation closer to the center of the sarcomere, in the region of the sarcomere regulated by MyBP-C. Thus, MyBP-C phospho-ablation would limit the recruitment of additional XBs in this region of the sarcomere following β-adrenergic signaling, thereby reducing the pool of recruitable XBs compared to the myofilaments expressing phosphorylatable MyBP-C. MyBP-C phosphorylation- and Ca²⁺-dependent regulation of XB recruitment could also explain the temporal pattern of enhanced pressure development following β-adrenergic signaling (Fig. 3). The recruitment of XBs not regulated by MyBP-C would produce an initial increase in pressure as cytosolic Ca²⁺ levels increase, followed by dobutamine-mediated acceleration of pressure development (observed after several milliseconds) due to recruitment of newly available XBs following MyBP-C phosphorylation to force-generating states.

Previously, it has been suggested that cardiac thick filaments harbor a subpopulation of super-relaxed (SRX) myosin heads that are characterized by substantially slower adenosine 5'-triphosphate (ATP) turnover rates (33, 34) and thereby equipping the cardiac contractile apparatus with a reserve of inactive myosin heads that can potentially be recruited into the force-bearing state under conditions of increased cardiac stress (35). Previous findings demonstrate that MyBP-C modulates the SRX state of myosin heads via its ability to interact with and position the myosin heads closer to the thick filament backbone and that a loss of MyBP-C decreases the number of SRX myosin heads (36). Thus, ablation of Ser³⁰² phosphorylation will potentially maintain the interactions of MyBP-C–SRX heads and possibly prevent them from being recruited toward the myosin binding sites on actin filaments, effectively reducing the number of XBs that can be recruited during thin filament activation. This suggests that a possible role of MyBP-C is to regulate the recruitable pool of XBs to fine-tune force generation during a cardiac twitch, with enhanced β-adrenergic signaling accelerating the initial rate of pressure development at higher workloads by increasing XB recruitment through MyBP-C Ser³⁰² phosphorylation. MyBP-C dephosphorylation limits this recruitable pool and prevents enhanced contraction in response to increased pacing or β-adrenergic signaling (7, 21), and loss of this regulation leads to altered timing of the cardiac cycle and a mismatch between ejection and filling (7).

CONCLUSIONS

Dephosphorylation of MyBP-C, and reduced Ser³⁰² phosphorylation (37, 38), in particular, has been documented in conditions of chronic human heart failure (HF) (37, 39), including patients exhibiting HF with preserved EF (HFpEF) (40), a detrimental condition caused by a complex interplay of deficits in both diastolic and systolic reserves (41). Notably, cardiac dysfunction in HFpEF is often not apparent at rest but becomes noticeable during stress or increased workloads, suggesting that an inability to modulate cardiac output leads to exercise intolerance in HFpEF patients (41). Myocardial samples isolated from HF patients also display desensitization of β-adrenergic signaling pathway (42) that produces a reduction in PKA-mediated phosphorylation of myofilament contractile proteins, including MyBP-C (37, 43). Recent evidence demonstrates that the loss of MyBP-C phosphorylation directly blunts enhanced myocardial force generation and ventricular pressure development in response to increased workloads (7, 21). Here,

we show that abolishing Ser³⁰² phosphorylation greatly diminishes the cardiac β -adrenergic reserve by blunting PKA-mediated enhancements in XB kinetics and dobutamine-mediated enhancements in systolic pressure generation, similar to the effects of abolishing all three PKA phosphorylation residues. These results establish MyBP-C Ser³⁰² as a critical modulator of cardiac output at higher workloads and suggest that therapeutic strategies designed to boost Ser³⁰² phosphorylation could be beneficial for contractile function and enhance cardiac output in HF patients with reduced cardiac β -adrenergic reserve.

MATERIALS AND METHODS

Ethical approval and animal treatment protocols

Experiments were conducted according to the procedures laid out in the *Guide for the Care and Use of Laboratory Animals* [National Institutes of Health (NIH) Publication No. 85-23, Revised 1996] and as per the guidelines of the Institutional Animal Care and Use Committee at the Case Western Reserve University. NTG wild-type mice expressing full-length MyBP-C and TG mice expressing nonphosphorylatable MyBP-C with Ser-to-Ala substitutions at Ser²⁷³, Ser²⁸², and Ser³⁰² (that is, TG^{35A}) (6, 16) were used as control groups. TG mice expressing MyBP-C with Ser-to-Ala substitution at Ser³⁰² (that is, TG^{S302A}) were generated on a MyBP-C-null background such that there is no endogenous Ser³⁰² phosphorylation. All mouse lines were of the SV/129 strain, and adult mice (3 to 6 months old) of both sexes were used for this study.

Determination of sarcomeric protein phosphorylation and MHC expression

Western blot and Pro-Q Diamond phosphoprotein stain (Life Technologies) were used to assess myofilament protein phosphorylation, as described previously (16, 44). On the day of the experiment, cardiac myofibrils were prepared by briefly homogenizing frozen mouse ventricular tissue for 15 s using a handheld homogenizer (PowerGen 500, Thermo Fisher Scientific) in relaxing solution that contains protease and phosphatase inhibitors (PhosSTOP and cOmplete ULTRA Tablets, Roche Applied Science). Myofibrils were chemically skinned for 15 min using 1% Triton X-100, centrifuged at 10,000g for 5 min, and resuspended in fresh relaxing solution on ice until further use. For PKA treatment, 100 μ g of myofibrils isolated from hearts of each mouse line was incubated with the catalytic subunit of bovine PKA (Sigma-Aldrich) to a final concentration of 0.15 U PKA/ μ g myofibrils for 1 hour at 30°C, and the reaction was stopped by the addition of Laemmli buffer (16). Control myofibrils were incubated under the same conditions without PKA. For Western blots, myofibrils were separated on 4 to 20% tris-glycine gels (Lonza), transferred to polyvinylidene difluoride (PVDF) membranes, and incubated overnight with one of the following primary antibodies: MyBP-C (Santa Cruz Biotechnology); MyBP-C phosphoserine 273, 282, or 302 (detects phosphorylation of Ser²⁷³, Ser²⁸², or Ser³⁰² of MyBP-C; 21st Century Biochemicals); or HSC70 as a loading control (Santa Cruz Biotechnology). PVDF membranes were then incubated with appropriate secondary antibodies and imaged. For estimating total myofilament protein phosphorylation, myofibrils were separated on 4 to 20% tris-glycine gels and stained with Pro-Q phosphostain. Pro-Q-stained gels were counterstained with Coomassie Blue to determine total protein content. Myocardial samples were run on 5% tris-HCl gels (Bio-Rad, #3450001), followed by staining with silver stain plus (Bio-Rad, #1610449) to quantify the MHC expression as β -MHC percentage of the total MHC expression in the sarcomere ($n = 6$ per group). MHC gels were run at 150 V for 4 hours at 4°C (6). Densito-

metric scanning of the stained gels was done using ImageJ software (NIH, Bethesda, MD) (16).

Histological analysis of cardiac tissue

To examine cardiac morphology, excised hearts were submerged in formalin for 4 hours and sectioned at the mid-LV, as previously described (7). Hearts were paraffin-embedded and sectioned at 5 μ m thickness before staining with Masson's trichrome.

Cardiac morphology, contractile function, and in vivo hemodynamic function

Cardiac morphology (that is, left ventricular wall thickness) and in vivo systolic (that is, EF) and diastolic (that is, IVRT) function were evaluated by echocardiography, as previously described (7). In vivo P-V loop analysis was used to evaluate hemodynamic function, as previously described (7, 16). For in vivo experiments, stable baseline measurements of maximal systolic pressure, end diastolic pressure, the maximum rate of systolic pressure development (dP/dt_{max}), and the time constant of diastolic pressure relaxation (τ) were made before intraperitoneal injection of dobutamine (10 μ g/g) to measure the response to increased β -adrenergic stimulation. P-V loops were analyzed offline using LabChart 7 software (ADInstruments).

Preparation of skinned myocardial preparations and Ca²⁺ solutions for mechanical experiments

Myocardial preparations were skinned, as previously described (16). In brief, frozen ventricular tissue pieces were homogenized in a relaxing solution, followed by detergent skinning using 1% Triton X-100 (Thermo Scientific) for 1 hour. Multicellular ventricular preparations measuring \sim 100 μ m in width and \sim 400 μ m in length were selected for the mechanical experiments. The composition of Ca²⁺ activation solutions prepared for the experiments was based on a computer program (45) and established stability constants (46). Ca²⁺ solutions contained the following: 14.5 mM creatine phosphate, 7 mM EGTA, and 20 mM imidazole. The maximal activating solution (pCa 4.5; pCa = $-\log [Ca^{2+}]_{free}$) also contained 65.45 KCl, 7.01 CaCl₂, 5.27 MgCl₂, 4.81 ATP, whereas the relaxing solution (pCa 9.0) contained 72.45 mM KCl, 0.02 mM CaCl₂, 5.42 mM MgCl₂, 4.76 mM ATP. The pH and the ionic strength of the Ca²⁺ solutions were set to 7.0 and 180 mM, respectively. A range of pCa solutions (pCa 6.3 to 5.4) containing varying amounts of $[Ca^{2+}]_{free}$ were then prepared by mixing appropriate volumes of pCa 9.0 and 4.5. stock solutions, and the mechanical experiments were performed at 23°C.

Experimental setup for measurement of dynamic and steady-state contractile properties in skinned myocardium

Detergent-skinned multicellular ventricular preparations were attached between a motor arm (312C, Aurora Scientific Inc.) and a force transducer (403A, Aurora Scientific Inc.), as described previously (47). Changes in the motor arm position and force transducer signals were sampled at 2000 Hz using a custom-built sarcomere length (SL) control software program developed by Campbell and Moss (48). For all mechanical measurements, SL of the ventricular preparations was set to 2.1 μ m (16). Force-pCa relationships were determined by incubating the skinned myocardial preparations in pCa solutions ranging from pCa 6.3 to 4.5. The apparent cooperativity of force generation was estimated from the steepness of Hill plot transformation of the force-pCa relationships (44). The force-pCa data were fit using the equation $P/P_0 = [Ca^{2+}]^{n_H} / (k^{n_H} + [Ca^{2+}]^{n_H})$, where n_H is the Hill coefficient and k is the pCa needed to elicit half-maximal force (that is, pCa₅₀) (44).

Stretch activation experiments to measure dynamic XB contractile parameters

The stretch activation protocol used in these studies was described earlier (3, 16, 49). Skinned myocardial preparations were placed in Ca^{2+} solutions (pCa 6.1) that generate ~35% of the maximal force. Once the preparations attained a steady-state force, they were rapidly stretched by 2% of their initial ML, held at the new ML for 8 s, and then returned back to their initial ML. The key features of the stretch activation responses in cardiac muscle have been described earlier (50, 51), and various stretch activation parameters measured are illustrated in Fig. 4A. In brief, a sudden 2% stretch in ML causes an instantaneous spike in the force response (P1), which is due to the sudden strain of elastic elements within the strongly bound XBs (phase 1). The force then rapidly decays (phase 2) because of the detachment of the strained XBs into a non-force-bearing state, with a dynamic rate constant k_{rel} (an index of XB detachment). The lowest point of phase 2 (nadir) is indicated by P2 and is an index of the magnitude of XB detachment. Following phase 2, the preparations exhibit a gradual rise of force (phase 3), with a dynamic rate constant k_{df} (an index of the rate of XB recruitment). The delayed force rise in phase 3 is due to the sudden stretch-mediated recruitment of new XBs into the force-bearing state (50, 51). Stretch activation amplitudes, P3 and P_{df} , were normalized to prestretch Ca^{2+} -activated force where P3 was measured from prestretch steady-state force to the peak force value of the delayed force attained in phase 3, whereas P_{df} was measured as the difference between P3 and P2 values, as described previously (3, 4, 47).

k_{rel} was measured by fitting a single exponential equation to the time course of force decay using the equation: $F(t) = a(-1 + \exp(-k_{\text{rel}}*t))$, where “a” is the amplitude of the single exponential phase and k_{rel} is the rate constant of the force decay, as done earlier (5). k_{df} , which represents the rate of recruitment of all XBs that give rise to the delayed force transient following the sudden stretch in ML (that is, P_{df}), was estimated by linear transformation of the half-time of force redevelopment (5), that is, $k_{\text{df}} = 0.693/t_{1/2}$, where $t_{1/2}$ is the time (in milliseconds) taken from the nadir (that is, the point of force reuptake at the end of phase 2) to the point of half-maximal force in phase 3 of the force response, where maximal force is indicated by a plateau region of phase 3 (that is, P3) (Fig. 4A) (5).

Stretch activation experiments were repeated following incubation of the myocardial preparations with PKA. Because PKA treatment decreases myofilament Ca^{2+} sensitivity of force generation, we used a pCa solution with slightly higher $[\text{Ca}^{2+}]_{\text{free}}$ (pCa 6.0) to closely match the activation levels before PKA treatment, as done in earlier studies (5, 16).

Data analysis

Data were analyzed using two-way analysis of variance (ANOVA), and multiple pairwise comparisons were made using Fisher's least significant difference (Fisher's LSD) method, as previously reported (44). One-way ANOVA was used for analyzing the data reported for echocardiography experiments. Values are reported as means \pm SEM. The criterion for statistical significance was set at $P < 0.05$, and the asterisks in the figures and tables denote statistical significance using post hoc Fisher's LSD comparisons.

REFERENCES AND NOTES

- J. L. Garvey, E. G. Kranias, R. J. Solaro, Phosphorylation of C-protein, troponin I and phospholamban in isolated rabbit hearts. *Biochem. J.* **249**, 709–714 (1988).
- R. J. Solaro, A. J. G. Moir, S. V. Perry, Phosphorylation of troponin I and the inotropic effect of adrenaline in the perfused rabbit heart. *Nature* **262**, 615–617 (1976).
- J. E. Stelzer, J. R. Patel, R. L. Moss, Protein kinase A-mediated acceleration of the stretch activation response in murine skinned myocardium is eliminated by ablation of cMyBP-C. *Circ. Res.* **99**, 884–890 (2006).
- J. E. Stelzer, J. R. Patel, J. W. Walker, R. L. Moss, Differential roles of cardiac myosin-binding protein C and cardiac troponin I in the myofibrillar force responses to protein kinase A phosphorylation. *Circ. Res.* **101**, 503–511 (2007).
- R. Mamidi, K. S. Gresham, S. Verma, J. E. Stelzer, Cardiac myosin binding protein-C phosphorylation modulates myofilament length-dependent activation. *Front. Physiol.* **7**, 38 (2016).
- C. W. Tong, J. E. Stelzer, M. L. Greaser, P. A. Powers, R. L. Moss, Acceleration of crossbridge kinetics by protein kinase A phosphorylation of cardiac myosin binding protein C modulates cardiac function. *Circ. Res.* **103**, 974–982 (2008).
- K. S. Gresham, J. E. Stelzer, The contributions of cardiac myosin binding protein C and troponin I phosphorylation to β -adrenergic enhancement of in vivo cardiac function. *J. Physiol.* **594**, 669–686 (2016).
- T. Nagayama, E. Takimoto, S. Sadayappan, J. O. Mudd, J. G. Seidman, J. Robbins, D. A. Kass, Control of in vivo contraction/relaxation kinetics by myosin binding protein C: Protein kinase A phosphorylation-dependent and -independent regulation. *Circulation* **116**, 2399–2408 (2007).
- D. Barefield, S. Sadayappan, Phosphorylation and function of cardiac myosin binding protein-C in health and disease. *J. Mol. Cell Cardiol.* **48**, 866–875 (2010).
- W. Jia, J. F. Shaffer, S. P. Harris, J. A. Leary, Identification of novel protein kinase A phosphorylation sites in the M-domain of human and murine cardiac myosin binding protein-C using mass spectrometry analysis. *J. Proteome Res.* **9**, 1843–1853 (2010).
- M. J. Previs, S. Beck Previs, J. Gulick, J. Robbins, D. M. Warshaw, Molecular mechanics of cardiac myosin-binding protein C in native thick filaments. *Science* **337**, 1215–1218 (2012).
- M. J. Previs, J. Y. Mun, A. J. Michalek, S. B. Previs, J. Gulick, J. Robbins, D. M. Warshaw, R. Craig, Phosphorylation and calcium antagonistically tune myosin-binding protein C's structure and function. *Proc. Natl. Acad. Sci. U.S.A.* **113**, 3239–3244 (2016).
- M. J. Previs, B. L. Prosser, J. Y. Mun, S. B. Previs, J. Gulick, K. Lee, J. Robbins, R. Craig, W. J. Lederer, D. M. Warshaw, Myosin-binding protein C corrects an intrinsic inhomogeneity in cardiac excitation-contraction coupling. *Sci. Adv.* **1**, e1400205 (2015).
- S. C. Bardswell, F. Cuello, J. C. Kentish, M. Avkiran, cMyBP-C as a promiscuous substrate: Phosphorylation by non-PKA kinases and its potential significance. *J. Muscle Res. Cell Motil.* **33**, 53–60 (2012).
- F. Cuello, S. C. Bardswell, R. S. Haworth, E. Ehler, S. Sadayappan, J. C. Kentish, M. Avkiran, Novel role for p90 ribosomal S6 kinase in the regulation of cardiac myofilament phosphorylation. *J. Biol. Chem.* **286**, 5300–5310 (2011).
- K. S. Gresham, R. Mamidi, J. E. Stelzer, The contribution of cardiac myosin binding protein-c Ser282 phosphorylation to the rate of force generation and in vivo cardiac contractility. *J. Physiol.* **592**, 3747–3765 (2014).
- S. Sadayappan, J. Gulick, H. Osinska, D. Barefield, F. Cuello, M. Avkiran, V. M. Lasko, J. N. Lorenz, M. Maillet, J. L. Martin, J. H. Brown, D. M. Bers, J. D. Molkenstein, J. James, J. Robbins, A critical function for Ser-282 in cardiac Myosin binding protein-C phosphorylation and cardiac function. *Circ. Res.* **109**, 141–150 (2011).
- L. Xiao, Q. Zhao, Y. Du, C. Yuan, R. J. Solaro, P. M. Buttrick, PKC ϵ increases phosphorylation of the cardiac myosin binding protein C at serine 302 both in vitro and in vivo. *Biochemistry* **46**, 7054–7061 (2007).
- S. C. Bardswell, F. Cuello, A. J. Rowland, S. Sadayappan, J. Robbins, M. Gautel, J. W. Walker, J. C. Kentish, M. Avkiran, Distinct sarcomeric substrates are responsible for protein kinase D-mediated regulation of cardiac myofilament Ca^{2+} sensitivity and cross-bridge cycling. *J. Biol. Chem.* **285**, 5674–5682 (2010).
- D. W. Kuster, V. Sequeira, A. Najafi, N. M. Boontje, P. J. Wijnker, E. R. Witjas-Paalberends, S. B. Marston, C. G. dos Remedios, L. Carrier, J. A. A. Demmers, C. Redwood, S. Sadayappan, J. van der Velden, GSK3 β phosphorylates newly identified site in the proline-alanine-rich region of cardiac myosin-binding protein C and alters cross-bridge cycling kinetics in human: Short communication. *Circ. Res.* **112**, 633–639 (2013).
- C. W. Tong, X. Wu, Y. Liu, P. C. Rosas, S. Sadayappan, A. Hudmon, M. Muthuchamy, P. A. Powers, H. H. Valdivia, R. L. Moss, Phosphoregulation of cardiac inotropy via myosin binding protein-C during increased pacing frequency or β 1-adrenergic stimulation. *Circ. Heart Fail.* **8**, 595–604 (2015).
- S. Sadayappan, J. Gulick, H. Osinska, L. A. Martin, H. S. Hahn, G. W. Dorn II, R. Klevisky, C. E. Seidman, J. G. Seidman, J. Robbins, Cardiac myosin-binding protein-C phosphorylation and cardiac function. *Circ. Res.* **97**, 1156–1163 (2005).

23. B. M. Palmer, S. Sadayappan, Y. Wang, A. E. Weith, M. J. Previs, T. Bekyarova, T. C. Irving, J. Robbins, D. W. Maughan, Roles for cardiac MyBP-C in maintaining myofilament lattice rigidity and prolonging myosin cross-bridge lifetime. *Biophys. J.* **101**, 1661–1669 (2011).
24. D. M. Bers, S. Despa, Na/K-ATPase—An integral player in the adrenergic fight-or-flight response. *Trends Cardiovasc. Med.* **19**, 111–118 (2009).
25. K. Campbell, Rate constant of muscle force redevelopment reflects cooperative activation as well as cross-bridge kinetics. *Biophys. J.* **72**, 254–262 (1997).
26. R. L. Moss, D. P. Fitzsimons, J. C. Ralphe, Cardiac MyBP-C regulates the rate and force of contraction in mammalian myocardium. *Circ. Res.* **116**, 183–192 (2015).
27. B. A. Colson, J. R. Patel, P. P. Chen, T. Bekyarova, M. I. Abdalla, C. W. Tong, D. P. Fitzsimons, T. C. Irving, R. L. Moss, Myosin binding protein-C phosphorylation is the principal mediator of protein kinase A effects on thick filament structure in myocardium. *J. Mol. Cell Cardiol.* **53**, 609–616 (2012).
28. J. Y. Mun, M. J. Previs, H. Y. Yu, J. Gulick, L. S. Tobacman, S. Beck Previs, J. Robbins, D. M. Warshaw, R. Craig, Myosin-binding protein C displaces tropomyosin to activate cardiac thin filaments and governs their speed by an independent mechanism. *Proc. Natl. Acad. Sci. U.S.A.* **111**, 2170–2175 (2014).
29. B. A. Colson, T. Bekyarova, M. R. Locher, D. P. Fitzsimons, T. C. Irving, R. L. Moss, Protein kinase A-mediated phosphorylation of cMyBP-C increases proximity of myosin heads to actin in resting myocardium. *Circ. Res.* **103**, 244–251 (2008).
30. M. Gautel, O. Zuffardi, A. Freiburg, S. Labelit, Phosphorylation switches specific for the cardiac isoform of myosin binding protein-C: A modulator of cardiac contraction? *EMBO J.* **14**, 1952–1960 (1995).
31. G. Kunst, K. R. Kress, M. Gruen, D. Uttenweiler, M. Gautel, R. H. Fink, Myosin binding protein C, a phosphorylation-dependent force regulator in muscle that controls the attachment of myosin heads by its interaction with myosin S2. *Circ. Res.* **86**, 51–58 (2000).
32. A. Weisberg, S. Winegrad, Alteration of myosin cross bridges by phosphorylation of myosin-binding protein C in cardiac muscle. *Proc. Natl. Acad. Sci. U.S.A.* **93**, 8999–9003 (1996).
33. R. Cooke, The role of the myosin ATPase activity in adaptive thermogenesis by skeletal muscle. *Biophys. Rev.* **3**, 33–45 (2011).
34. M. A. Stewart, K. Franks-Skiba, S. Chen, R. Cooke, Myosin ATP turnover rate is a mechanism involved in thermogenesis in resting skeletal muscle fibers. *Proc. Natl. Acad. Sci. U.S.A.* **107**, 430–435 (2010).
35. J. W. McNamara, A. Li, G. C. dos Remedios, R. Cooke, The role of super-relaxed myosin in skeletal and cardiac muscle. *Biophys. Rev.* **7**, 5–14 (2015).
36. J. W. McNamara, A. Li, N. J. Smith, S. Lal, R. M. Graham, K. B. Kooiker, S. J. van Dijk, C. G. Remedios, S. P. Harris, R. Cooke, Ablation of cardiac myosin binding protein-C disrupts the super-relaxed state of myosin in murine cardiomyocytes. *J. Mol. Cell Cardiol.* **94**, 65–71 (2016).
37. O. Copeland, S. Sadayappan, A. E. Messer, G. J. Steinen, J. van der Velden, S. B. Marston, Analysis of cardiac myosin binding protein-C phosphorylation in human heart muscle. *J. Mol. Cell Cardiol.* **49**, 1003–1011 (2010).
38. V. Kooij, R. J. Holewinski, A. M. Murphy, J. E. Van Eyk, Characterization of the cardiac myosin binding protein-C phosphoproteome in healthy and failing human hearts. *J. Mol. Cell Cardiol.* **60**, 116–120 (2013).
39. A. M. Jacques, O. Copeland, A. E. Messer, C. E. Gallon, K. King, W. J. McKenna, V. T. Tsang, S. B. Marston, Myosin binding protein C phosphorylation in normal, hypertrophic and failing human heart muscle. *J. Mol. Cell Cardiol.* **45**, 209–216 (2008).
40. M. M. LeWinter, B. M. Palmer, Updating the physiology and pathophysiology of cardiac myosin-binding protein-C. *Circ. Heart Fail.* **8**, 417–421 (2015).
41. B. A. Borlaug, The pathophysiology of heart failure with preserved ejection fraction. *Nat. Rev. Cardiol.* **11**, 507–515 (2014).
42. M. R. Bristow, R. Ginsburg, W. Minobe, R. S. Cubicciotti, W. S. Sageman, K. Lurie, M. E. Billingham, D. C. Harrison, E. B. Stinson, Decreased catecholamine sensitivity and β -adrenergic-receptor density in failing human hearts. *N. Engl. J. Med.* **307**, 205–211 (1982).
43. R. Zaremba, D. Merkus, N. Hamdani, J. M. Lamers, W. J. Paulus, C. dos Remedios, D. J. Duncker, G. J. Stienen, J. van der Velden, Quantitative analysis of myofilament protein phosphorylation in small cardiac biopsies. *Proteomics Clin. Appl.* **1**, 1285–1290 (2007).
44. R. Mamidi, K. S. Gresham, J. E. Stelzer, Length-dependent changes in contractile dynamics are blunted due to cardiac myosin binding protein-C ablation. *Front. Physiol.* **5**, 461 (2014).
45. A. Fabiato, Computer programs for calculating total from specified free or free from specified total ionic concentrations in aqueous solutions containing multiple metals and ligands. *Methods Enzymol.* **157**, 378–417 (1988).
46. R. E. Godt, B. D. Lindley, Influence of temperature upon contractile activation and isometric force production in mechanically skinned muscle fibers of the frog. *J. Gen. Physiol.* **80**, 279–297 (1982).
47. R. Mamidi, K. S. Gresham, A. Li, C. G. dos Remedios, J. E. Stelzer, Molecular effects of the myosin activator omecamtiv mecarbil on contractile properties of skinned myocardium lacking cardiac myosin binding protein-C. *J. Mol. Cell Cardiol.* **85**, 262–272 (2015).
48. K. S. Campbell, R. L. Moss, SLControl: PC-based data acquisition and analysis for muscle mechanics. *Am. J. Physiol. Heart Circ. Physiol.* **285**, H2857–H2864 (2003).
49. S. K. Gollapudi, R. Mamidi, S. L. Mallampalli, M. Chandra, The N-terminal extension of cardiac troponin T stabilizes the blocked state of cardiac thin filament. *Biophys. J.* **103**, 940–948 (2012).
50. S. J. Ford, M. Chandra, R. Mamidi, W. Dong, K. B. Campbell, Model representation of the nonlinear step response in cardiac muscle. *J. Gen. Physiol.* **136**, 159–177 (2010).
51. J. E. Stelzer, J. R. Patel, R. L. Moss, Acceleration of stretch activation in murine myocardium due to phosphorylation of myosin regulatory light chain. *J. Gen. Physiol.* **128**, 261–272 (2006).

Acknowledgments

Funding: This work was supported by the NIH (HL-114770 and P30 EY011373 to J.E.S.) and the American Heart Association (16POST30730000 to R.M.) grants. **Author contributions:** R.M., K.S.G., and J.E.S. contributed to the conception and design of the experiments. R.M., K.S.G., J.L., and J.E.S. participated in performing the experiments, in acquiring, analyzing, and interpreting data, and in drafting and revising the manuscript. All authors approved the final version of the manuscript. **Competing interests:** The authors declare that they have no competing interests. **Data and materials availability:** All data needed to evaluate the conclusions in the paper are present in the paper. Additional data related to this paper may be requested from the authors.

Submitted 6 October 2016

Accepted 2 February 2017

Published 10 March 2017

10.1126/sciadv.1602445

Citation: R. Mamidi, K. S. Gresham, J. Li, J. E. Stelzer, Cardiac myosin binding protein-C Ser³⁰² phosphorylation regulates cardiac β -adrenergic reserve. *Sci. Adv.* **3**, e1602445 (2017).

This article is published under a Creative Commons license. The specific license under which this article is published is noted on the first page.

For articles published under [CC BY](#) licenses, you may freely distribute, adapt, or reuse the article, including for commercial purposes, provided you give proper attribution.

For articles published under [CC BY-NC](#) licenses, you may distribute, adapt, or reuse the article for non-commercial purposes. Commercial use requires prior permission from the American Association for the Advancement of Science (AAAS). You may request permission by clicking [here](#).

The following resources related to this article are available online at <http://advances.sciencemag.org>. (This information is current as of March 28, 2017):

Updated information and services, including high-resolution figures, can be found in the online version of this article at:

<http://advances.sciencemag.org/content/3/3/e1602445.full>

This article **cites 51 articles**, 25 of which you can access for free at:

<http://advances.sciencemag.org/content/3/3/e1602445#BIBL>

Science Advances (ISSN 2375-2548) publishes new articles weekly. The journal is published by the American Association for the Advancement of Science (AAAS), 1200 New York Avenue NW, Washington, DC 20005. Copyright is held by the Authors unless stated otherwise. AAAS is the exclusive licensee. The title *Science Advances* is a registered trademark of AAAS